Developmental Apoptosis Mediates Entry and Positioning of Microglia in the Zebrafish Brain

Casano, Alessandra Maria ; Albert, Marvin ; Peri, Francesca

Abstract: In the brain, neurons that fail to assemble into functional circuits are eliminated. Their clearance depends on microglia, immune cells that colonize the CNS during embryogenesis. Despite the importance of these cells in development and disease, the mechanisms that target and position microglia within the brain are unclear. Here we show that, in zebrafish, attraction of microglia into the brain exploits differences in developmental neuronal apoptosis and that these provide a mechanism for microglial distribution. Reducing neuronal cell death results in fewer microglia, whereas increased apoptosis enhances brain colonization, resulting in more microglia at later stages. Interestingly, attraction into the brain depends on nucleotide signaling, the same signaling system used to guide microglia toward brain injuries. Finally, this work uncovers a cell-non-autonomous role for developmental apoptosis. Classically considered a wasteful process, programmed cell death is exploited here to configure the immune-neuronal interface of the brain.

DOI: https://doi.org/10.1016/j.celrep.2016.06.033

Cell Reports

Report

Developmental Apoptosis Mediates Entry and Positioning of Microglia in the Zebrafish Brain

Graphical Abstract

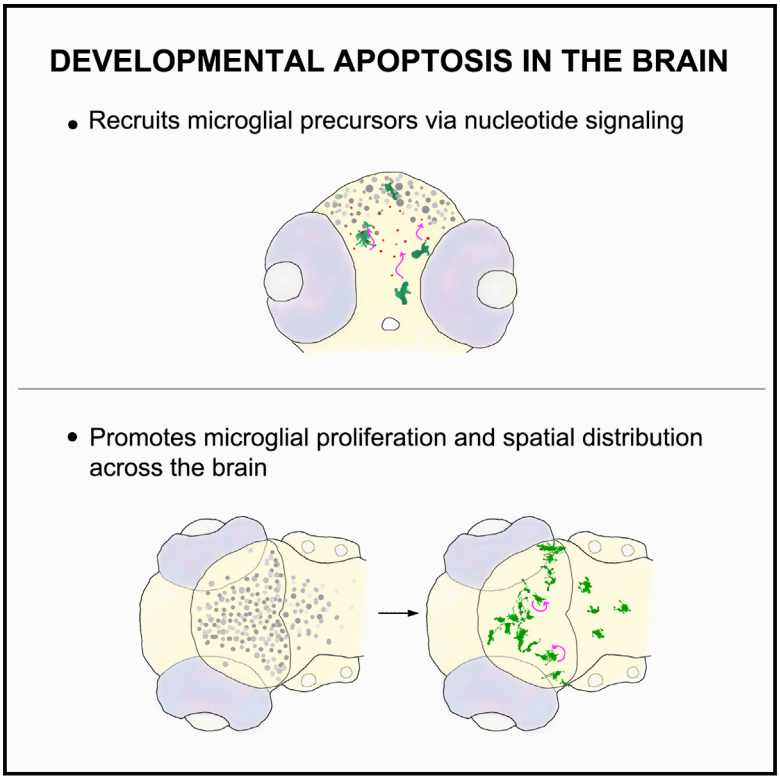

Highlights

- Neuronal apoptosis attracts committed microglial precursors into the brain
- Apoptosis-driven attraction depends on nucleotide signaling
- Developmental apoptosis configures the immune-neuronal interface of the brain

Authors

Alessandra Maria Casano, Marvin Albert, Francesca Peri

Correspondence

peri@embl.de

In Brief

Casano et al. show that establishment of the microglial population is linked to developmental apoptosis in the brain. Differences in neuronal apoptosis provide a mechanism for entry and positioning of microglial precursors within the brain. Attraction is mediated by nucleotide signaling previously shown to guide microglia toward brain injuries.

Casano et al., 2016, Cell Reports *16*, 897–906
July 26, 2016
http://dx.doi.org/10.1016/j.celrep.2016.06.033

CellPress

Cell Reports
Report

Developmental Apoptosis Mediates Entry and Positioning of Microglia in the Zebrafish Brain

Alessandra Maria Casano,[1] Marvin Albert,[1] and Francesca Peri[1,*]
[1]Developmental Biology Unit, European Molecular Biology Laboratory (EMBL), Meyerhofstrasse 1, 69117 Heidelberg, Germany
*Correspondence: peri@embl.de
http://dx.doi.org/10.1016/j.celrep.2016.06.033

SUMMARY

In the brain, neurons that fail to assemble into functional circuits are eliminated. Their clearance depends on microglia, immune cells that colonize the CNS during embryogenesis. Despite the importance of these cells in development and disease, the mechanisms that target and position microglia within the brain are unclear. Here we show that, in zebrafish, attraction of microglia into the brain exploits differences in developmental neuronal apoptosis and that these provide a mechanism for microglial distribution. Reducing neuronal cell death results in fewer microglia, whereas increased apoptosis enhances brain colonization, resulting in more microglia at later stages. Interestingly, attraction into the brain depends on nucleotide signaling, the same signaling system used to guide microglia toward brain injuries. Finally, this work uncovers a cell-non-autonomous role for developmental apoptosis. Classically considered a wasteful process, programmed cell death is exploited here to configure the immune-neuronal interface of the brain.

INTRODUCTION

Programmed cell death is the driving force behind the development of many organs including the brain. According to the neurotropic theory, competition for limited amount of survival factors leads to the death of many neurons (for reviews see Dekkers et al. [2013] and Nijhawan et al. [2000]). Clearance of apoptotic corpses in the developing brain relies on phagocytic microglia, the resident macrophages of the vertebrate CNS. Lineage-tracing studies in mouse have revealed that these cells derive from erythromyeloid precursors (EMPs) that invade the CNS during early development and are maintained in the adult by local proliferation (Ginhoux et al., 2010; Kierdorf et al., 2013; Gomez Perdiguero et al., 2015). The hematopoietic embryonic origin of microglial cells is conserved across vertebrate species (Ginhoux et al., 2013). For instance, in zebrafish, embryonic macrophages are produced both at 20 and 30 hr postfertilization (hpf) in the anterior lateral plate mesoderm (ALPM) and in the intermediate cell mass (ICM), respectively (Stachura and Traver, 2011; Xu et al., 2012). Brain colonization starts at 48 hpf, when few ALPM-derived macrophages enter the brain parenchyma (Herbomel et al., 2001; Rossi et al., 2015). In addition, recent work has shown that, at 14 days postfertilization (dpf), there is a second wave of ventral dorsal aorta (VDA)-derived macrophages contributing to the establishment of the microglial adult pool (Xu et al., 2015).

Although the myeloid origin of these cells is widely accepted, the dynamics of microglial brain colonization remain elusive; for instance, it is unclear whether targeting to the brain is random or if hardwired pre-patterned signals guide microglial cells. The recent identification of *slc7a7*$^{+}$ microglial precursors in zebrafish (Rossi et al., 2015) and the requirement for CXCL12 and CX3CL1 in positioning mouse microglia (Arnò et al., 2014; Hoshiko et al., 2012) point toward the existence of active mechanisms to ensure microglial brain colonization. Given that the number and distribution of microglia in the adult also have been shown to influence learning and behavior (Chen et al., 2010; Parkhurst et al., 2013), uncovering the mechanisms that target and position microglia during development is of significant biological and medical interest.

Here, we take advantage of live imaging in zebrafish to investigate the dynamics of microglial colonization during embryogenesis. In particular, we demonstrate that attraction and positioning of these cells exploit a physiological feature of brain development, namely, naturally occurring neuronal apoptosis, uncovering a direct link between cell death and homing of tissue-resident macrophages.

RESULTS

Spatial and Temporal Correlations between Neuronal Apoptosis and Microglial Brain Colonization during Embryonic Development

To investigate the dynamics of microglial brain colonization, we first took an in vivo imaging approach. By tracking macrophages at high spatial and temporal resolutions between 2 and 3 dpf, we found that both macrophage invasion and local proliferation contribute to the establishment of the microglial population (Figures 1A–1C; Movie S1). We then quantified these two processes by performing a series of pulse-chase experiments using a

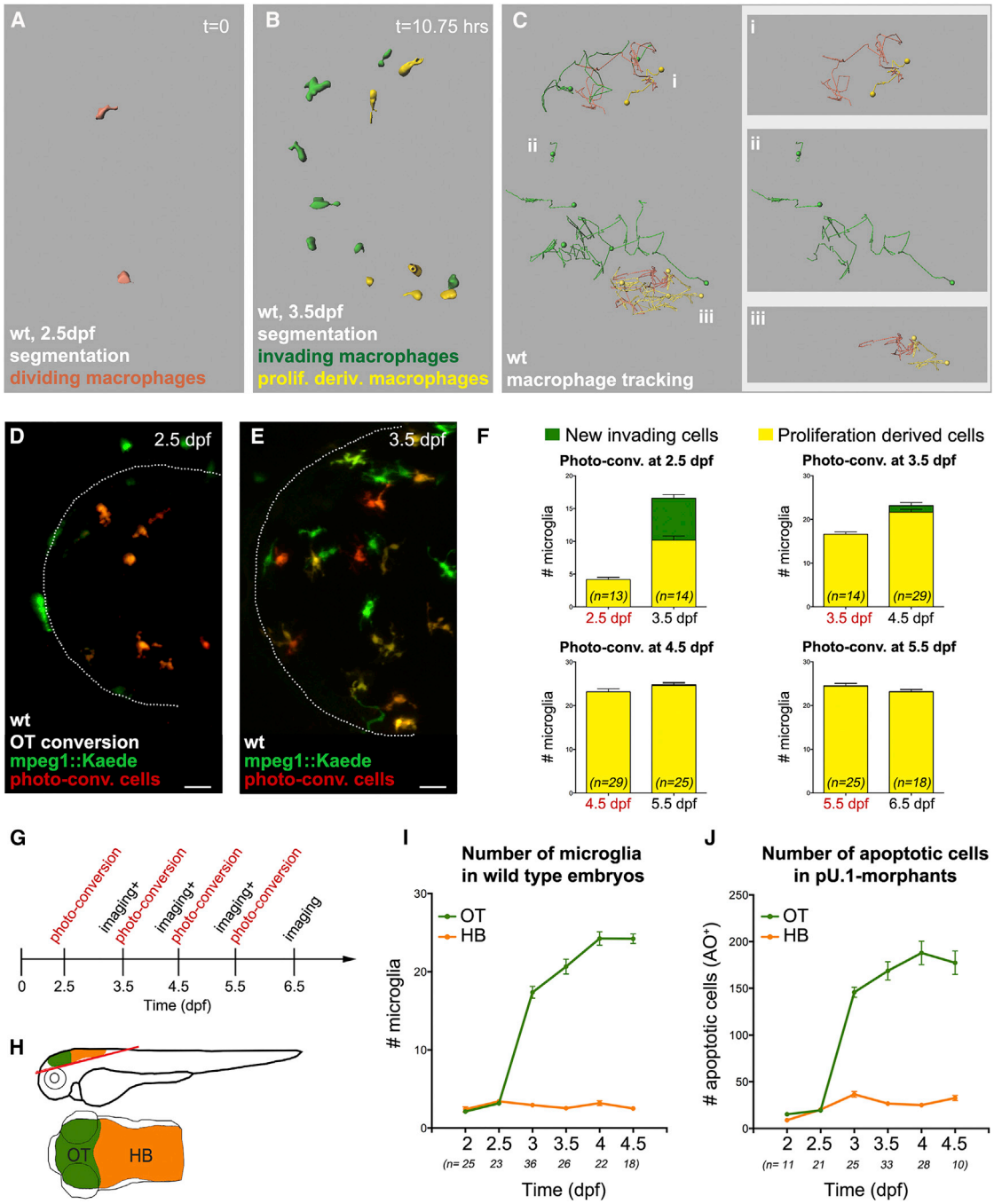

Figure 1. Dynamics of Microglial Brain Colonization and Neuronal Apoptosis

(A–C) Macrophage cell segmentation (A [t = 0 hr] and B [t = 10.75 hr]) and cell tracking (C) of a representative wild-type *mpeg1*::*GAL4-UAS*::*Kaede* embryo, imaged for 10.75 hr (Movie S1). In orange are the proliferating and in green are the invading macrophages/tracks. Yellow marks cells resulting from division. Examples of single tracks are given in (i), (ii), and (iii).

(D and E) Dorsal view of a *mpeg1*::*GAL4-UAS*::*Kaede* embryo after microglia photo-conversion (D) and 24 hr later (E). Microglia that entered the brain after photo-conversion are green. Microglia derived from proliferating converted cells are in red/yellow. Dotted lines mark the tectal area.

(F) Quantifications of microglial photo-conversion at different developmental time points. In each graph, the histogram on the left represents the number of microglia photo-converted at a given time point (in red). The histogram on the right indicates the number of microglia entering the brain after conversion (green bar) or deriving from proliferation (yellow bar) 24 hr after photo-conversion.

(G) Experimental setup. Microglia are photo-converted at different time points. Then, 24 hr after each round of photo-conversion, green and red/yellow cells are quantified.

(legend continued on next page)

transgenic line where macrophages express the photo-convertible protein Kaede, which allows macrophages in the brain to be photo-converted from green to red (Figures 1D and 1G; Ellett et al., 2011; Svahn et al., 2013). Counting the number of red/yellow cells 24 hr later allows quantification of the rate of in loco proliferation (Figures 1E and 1F, yellow bars). We next determined the rate of brain invasion by quantifying green cells that arrived into the brain after photo-conversion (Figures 1E and 1F, green bars). Monitoring these populations independently during the first 6 days of development revealed that both invasion and in loco proliferation equally contribute to microglial brain colonization and peak between 2 and 3 dpf (Figure 1F), indicating that key regulatory events take place at this stage.

Interestingly, when we compared microglial cell numbers in two neighboring brain regions, the optic tectum and the hindbrain (Figure 1H), we found that these are characterized by different colonization rates. Indeed, the optic tectum shows more microglia than the hindbrain (Figures 1I, S1A, S1B, S1D, S1E, S1G, and S1H), a differential that also is observed in adults (Svahn et al., 2013). Given that one of the functions of microglia at this stage is the engulfment of apoptotic neurons (Casano and Peri, 2015; Mazaheri et al., 2014; Sierra et al., 2013), we next asked whether microglial distribution correlates with differences in physiological patterns of developmental neuronal cell death. Thus, we quantified the absolute numbers of apoptotic neurons between 2 and 4 dpf in brains that lack phagocytic microglia (Rhodes et al., 2005), and we found a positive spatiotemporal correlation between patterns of neuronal apoptosis and microglial distribution (compare Figures 1J, 1I, S1C, S1F, and S1I), suggesting a possible mechanistic link between these two processes.

Altering the Rate of Neuronal Apoptosis Changes the Number of Microglia in the Brain

To test a causal role for developmental neuronal cell death in determining the size of the microglial population, we developed methods to quantify microglia after altering levels of apoptosis in the brain. First, we decreased neuronal cell death prior to microglial colonization by combining *caspase-3* knockdown with the caspase inhibitor Z-VAD-fmk (Yamashita et al., 2008; Williams and Holder, 2000). This resulted in a 50% reduction in the number of apoptotic neurons, as shown by acridine orange (AO) staining (Figures 2A, 2B, and 2D), and a concomitant decrease in the number of microglia (Figures 2E, 2F, and 2H), without affecting the number of macrophages elsewhere (Figures S1J–S1L). Similar results also were obtained by reducing cell death in the brain via neuronal overexpression of the inhibitor of apoptosis *xiap* (Deveraux et al., 1997; Figures 2C, 2D, 2G, 2H, S1M, and S1N).

Next, we developed protocols for increasing brain apoptosis by applying low-power UV laser irradiation in 3-day-old embryos. Here only one brain hemisphere was irradiated, leaving the non-irradiated hemisphere as an internal control. AO staining confirmed that the number of apoptotic nuclei in the brain increased significantly after UV laser irradiation when compared to the control hemisphere (Figures S2A–S2C and S2G). Similarly, the number of microglia was higher in irradiated hemispheres than in control sides (Figure S2H). We performed the same single-hemisphere UV treatment on *p53*-morphant embryos where UV-mediated apoptosis is impaired (Rentzsch et al., 2003). As both treated and un-treated hemispheres had comparable numbers of both dead neurons and microglia (Figures S2D–S2H), we concluded that changes in microglial cell numbers depend on UV-induced neuronal apoptosis. Altogether these experiments suggest that neuronal apoptosis provides a mechanism for controlling the number of microglia in the brain.

Ectopic Neuronal Apoptosis Influences Microglial Colonization and Distribution within the Brain

Next we wanted to determine whether neuronal cell death defines a pattern for microglia positioning. To this aim, we generated an ectopic domain of apoptosis within the hindbrain, a brain region that is normally characterized by low numbers of dying neurons. This was achieved using a zebrafish line in which the bacterial nitroreductase (NTR) fused to mCherry is expressed in the hindbrain (*nbt::DlexPR-lexOP::NTR-mCherry;* referred to as *HB-NTR-mCherry*). As previously reported, this system allows transient Caspase-3-dependent cell ablation of labeled cells upon the addition of metronidazole (MTZ; Curado et al., 2007; Pisharath et al., 2007; van Ham et al., 2014). Importantly, expression alone or administration of MTZ to non-transgenic embryos did not induce apoptosis or change microglial distribution within the brain (Figures S3A–S3C and S3E). By contrast, a single pulse of MTZ (Figure 2P) was sufficient to boost neuronal death in the hindbrain of *HB-NTR-mCherry* embryos (compare Figures S3C and S3D). This resulted in a significant increase in the number of hindbrain microglia 24 hr after treatment (Figures 2I, 2J, S3E, and S3F).

Interestingly, 1 week after, while the apoptotic stimulus had ceased (Figures S3G and S3H) and most NTR-mCherry^{+} neurons had been removed (Figure 2M), the number of microglia in the hindbrain was still high (Figures 2K–2M). To determine whether this was due to the fact that the additional microglia maintain their position in the hindbrain, we combined MTZ treatments with hindbrain microglia photo-conversion 24 hr after the induction of apoptosis (Figure 2P). Imaging 1 week after photo-conversion showed that both MTZ-treated and control embryos had few newly arrived microglia; however, in MTZ-treated samples, most microglia were red/yellow, indicating that in response to the apoptotic stimulus these cells remained in the hindbrain (Figures 2N, 2O, S3I, and S3J).

To further characterize this increase in microglial cell number, we allowed MTZ-treated *HB-NTR-mCherry* embryos to develop until juvenile stages, and we quantified microglia in the medulla, a hindbrain-derived region, using an antibody against L-plastin (Kizil et al., 2012; Kroehne et al., 2011). Interestingly, we found

(H) Schematic illustrations of a 3-dpf embryo (side and dorsal views). The red line marks the depth at which confocal imaging was performed.
(I and J) Quantifications of the number of microglia (I) and apoptotic nuclei (J) in wild-type and *pU.1*-morphant brains, respectively, are shown.
OT, optic tectum; HB, hindbrain; AO, acridine orange; n, number of embryos. For all quantifications, data are pooled from three independent experiments. Scale bar represents 30 μm. See also Figure S1 and Movie S1.

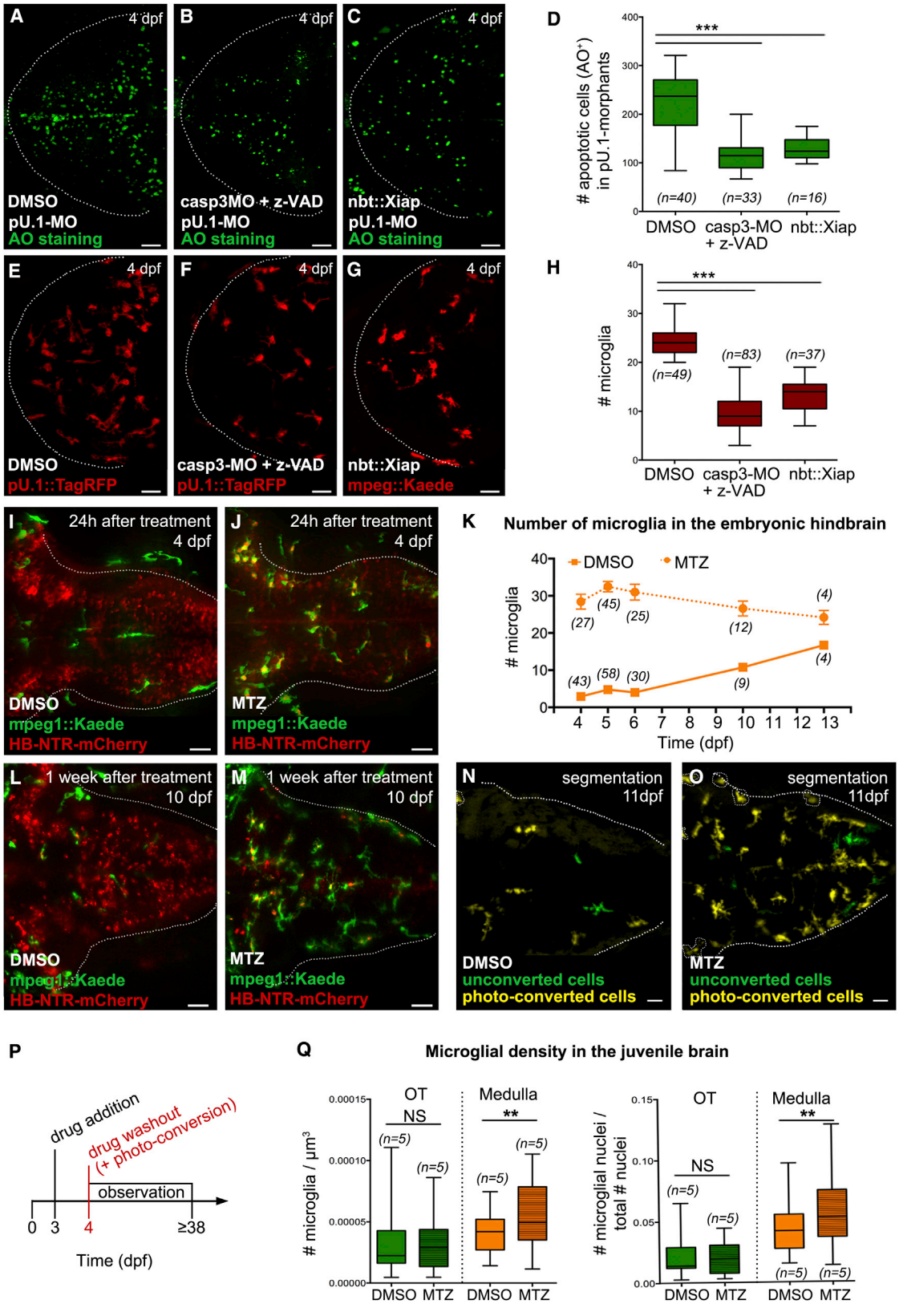

(legend on next page)

that microglial numbers were increased in transgenic fish treated with a single pulse of MTZ compared to controls (Figures 2Q and S3O, graphs in orange). Notably, in brain areas not affected by the MTZ treatment, such as the optic tectum, microglial distribution was unaltered (Figures 2Q and S3O, graphs in green). Altogether, these results establish a clear link between neuronal death in the embryo and microglial distribution at later stages, indicating that both levels and patterns of developmental brain apoptosis have a strong and prolonged influence on microglial distribution within the brain.

Developmental Neuronal Cell Death Recruits Microglial Precursors into the Brain via Nucleotide Signaling

Developmental neuronal apoptosis could regulate the number of microglia in the brain either by controlling how many macrophages enter and/or by promoting their proliferation in loco. To distinguish between these mechanisms, we combined NTR treatment of *HB-NTR-mCherry* embryos with photo-conversion of hindbrain Kaede^{+} macrophages (Figures 3C and 3D). Imaging 24 hr after photo-conversion revealed that, upon inducing apoptosis, a large number of green unconverted cells accumulate in the hindbrain, whereas the number of microglia remained unchanged in control samples (Figures 3E–3G). This indicates that increased neuronal apoptosis enhances microglial hindbrain invasion. To further test this point, we combined ectopic apoptosis in the hindbrain with the photo-conversion of macrophages located in a defined ventral region outside the brain (Figure 3H). As a result, red/yellow photo-converted cells accumulated in the hindbrain (Figures 3I–3K). Importantly, these additional cells were positive for *slc7a7*, a marker for microglial precursors in zebrafish (Rossi et al., 2015; Figures 3A and 3B). Thus, we can conclude that neuronal apoptosis provides a stimulus for the recruitment of macrophages that are committed to the microglial lineage.

To further probe apoptosis-driven attraction of microglial precursors to the brain, we investigated the role of nucleotide signaling, which has been shown to attract phagocytes toward apoptotic cells (Elliott et al., 2009; Chekeni et al., 2010; Sandilos et al., 2012). The nucleotide-signaling pathway was blocked via two complementary strategies: impairing nucleotide release via morpholino knockdown of *pannexin-1a* (Li et al., 2012) and using the drug inhibitor carbenoxolone (CBX). In addition, we blocked detection of nucleotides on macrophages by applying suramin, a broad purinergic receptor inhibitor (von Kügelgen, 2008). Neither treatment affected levels of neuronal death (Figures 4A–4E) nor did they impair the distribution and basal motility of macrophages outside the brain (Figures S3K–S3N, S3R, and S3U); however, they significantly reduced the number of microglia (Figures 4F–4J, S3P, S3Q, S3S, and S3T). Interestingly, this phenotype was observed only when embryos were treated before or during brain colonization (Figures S4A–S4D and S4L), and normal microglial numbers were rapidly reestablished by washing out these inhibitors during this time (Figures S4E–S4H). This indicates that microglial decrease is not due to non-specific toxicity or a general defect in cell movement but is consistent with nucleotide signaling being responsible for the attraction of macrophages into the brain. In addition, these treatments suppressed the microglial increase observed in HB-NTR-mCherry embryos following the induction of ectopic hindbrain apoptosis (Figures 4K–4N).

Combining administration of suramin or CBX with in vivo live imaging and photo-conversion of Kaede^{+} microglia revealed that nucleotide signaling influences microglial amounts by specifically regulating the number of macrophages that enter into the brain, leaving the rate of in loco proliferation unaltered (Figures 4O–4S). This was confirmed by monitoring microglial precursors in the *slc7a7*::*Kaede* line (Rossi et al., 2015). Indeed, upon blocking nucleotide signaling, there were fewer *slc7a7*$^{+}$ precursor cells in the optic tectum, while many were found anteriorly in a position that was previously identified as the migratory path to the brain (Rossi et al., 2015; Figure 4T, graph on the left; Figures S4M–S4O). Interestingly, 24 hr after drug washout, normal microglial distribution was restored (Figure 4T, graph on the right; Figures S4P–S4R). To prove that this was due to the migration of macrophages from the anterior into the brain, we photo-converted cells that were trapped anteriorly, washed out the nucleotide signaling inhibitors, and imaged the optic tectum 1 day later. The presence of red/yellow microglia

Figure 2. Neuronal Cell Death Affects Size and Distribution of the Microglial Population

(A–D) AO staining (A–C) and quantifications (D) of apoptotic nuclei in 4-dpf *pU.1*-morphant embryos treated with DMSO (A), *caspase-3*-morpholino + z-VAD-fmk (B), and neuronal *xiap* overexpression (C) are shown.

(E–H) Distribution (E–G) and quantification (H) of microglia in the optic tectum of 4-dpf *pU.1*::*GAL4-UAS*::*TagRFP* and *mpeg1*::*GAL4-UAS*::*Kaede* embryos treated with DMSO (E), *caspase-3*-morpholino + z-VAD-fmk (F), and neuronal *xiap* overexpression (G) are shown.

(I, J, L, and M) Hindbrain dorsal views of an *mpeg1*::*GAL4-UAS*::*Kaede*;*HB-NTR-mCherry* embryo 24 hr (I and J) and 1 week (L and M) after treatment with DMSO or MTZ are shown.

(K) Quantification of hindbrain microglia in *mpeg1*::*GAL4-UAS*::*Kaede*;*HB-NTR-mCherry* embryos, at different time points after pulsed treatment with DMSO or MTZ. Numbers indicate how many embryos have been analyzed.

(N and O) Manual segmentation of photo-converted microglia (yellow cells) and new invading macrophages (green cells) in the hindbrain of a representative *mpeg1*::*GAL4-UAS*::*Kaede*;*HB-NTR-mCherry* larva 1 week after pulse of DMSO or MTZ and hindbrain microglia photo-conversion (original data in Figures S3I and S3J). NTR-mCherry^{+} neurons are omitted. Macrophages located superficially in the skin, outside the brain, are encircled with a white dotted line.

(P) Experimental setup. At 3 dpf, NTR-mCherry^{+} embryos are treated with DMSO or MTZ. Then 24 hr later the drug is removed and hindbrain microglia are photo-converted. Microglia in the hindbrain are quantified at different developmental time points.

(Q) Accumulation of microglia in the optic tectum and medulla oblongata of *mpeg1*::*GAL4-UAS*::*Kaede*;*HB-NTR-mCherry* juvenile fish, ~1 month after DMSO or MTZ treatment. Microglial densities are calculated as the number of microglia/micron^3 or as the ratio between the number of microglia and the total number of nuclei.

AO, acridine orange; OT, optic tectum; n, number of embryos or fish; NS, non-significant; $^{**}p < 0.01$ and $^{***}p < 0.001$. Dotted lines delimit the regions of interest. For all quantifications, data are pooled from three independent experiments. Scale bar represents 30 μm. See also Figures S1, S2, and S3.

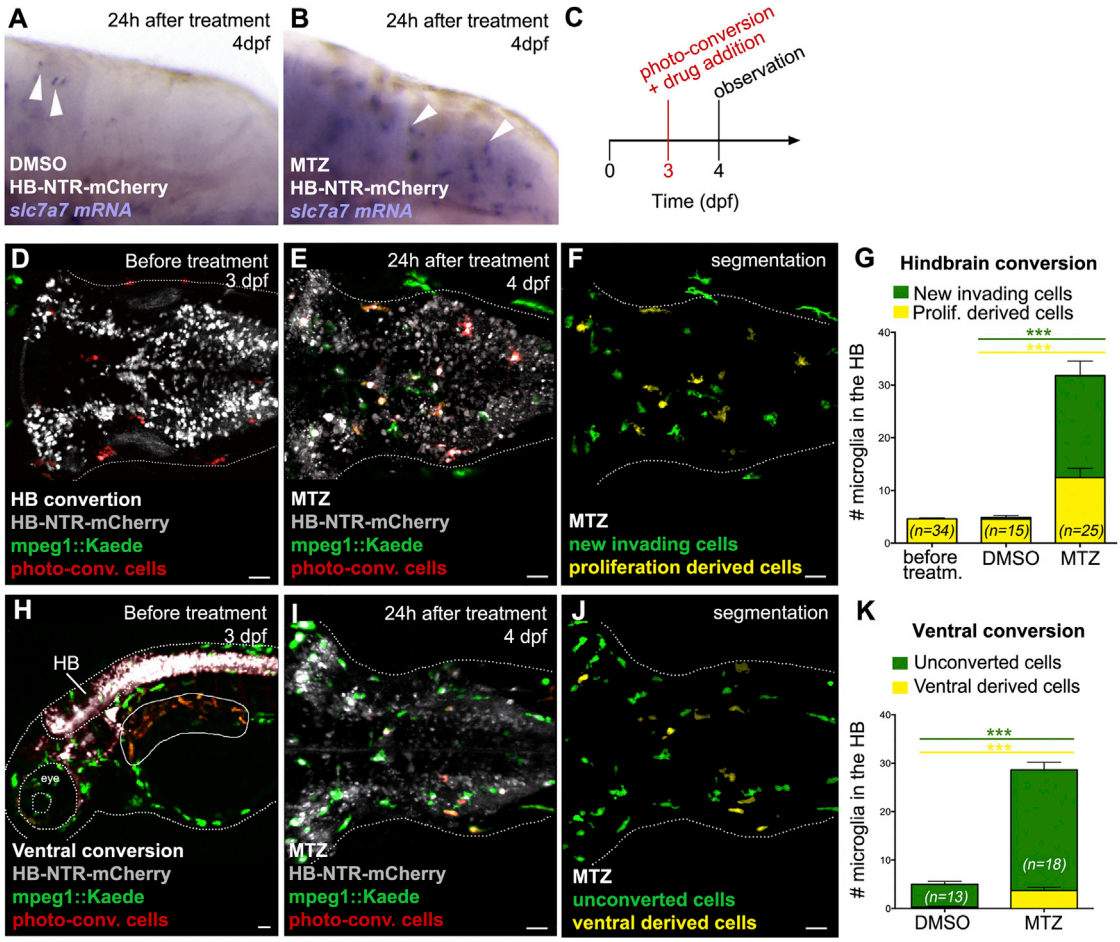

Figure 3. Neuronal Apoptosis Promotes Microglial Brain Colonization by Attracting Macrophages into the Brain

(A and B) Whole mount in situ hybridization (WISH) images show *slc7a7* expression (white arrowheads) in *HB-NTR-mCherry* transgenic embryos 24 hr after DMSO (A) or MTZ (B) treatment.

(C) Experimental setup. At 3 dpf, Kaede^{+} cells are photo-converted in the hindbrain or ventral region of NTR-mCherry^{+} embryos and soon after samples are treated with DMSO or MTZ. Then 24 hr later green and red/yellow cells are quantified in the hindbrain.

(D and E) Hindbrain dorsal views of a 3-dpf *mpeg1*::*GAL4-UAS*::*Kaede*;*HB-NTR-mCherry* embryo, after microglia photo-conversion and prior to drug treatment (D) and 24 hr after photo-conversion and MTZ treatment (E). New invading microglia are in green and microglia derived from converted cells are in red/yellow.

(F and J) Segmented images of (E) and (I), respectively. NTR-mCherry^{+} neurons are omitted.

(G) Quantification of hindbrain microglia after induction of apoptosis. Histogram on the left refers to the number of photo-converted microglia populating the hindbrain prior to MTZ incubation; histograms on the right represent the number of newly arrived microglia (green bars) and those resulting from local proliferation (yellow bars) 24 hr after photo-conversion and DMSO or MTZ treatment. Data are from three independent experiments.

(H) Lateral view shows a 3-dpf *mpeg1*::*GAL4-UAS*::*Kaede*;*HB-NTR-mCherry* embryo, after photo-conversion of Kaede^{+} macrophages in the ventral region (red cells, solid line) and before MTZ treatment.

(I) Hindbrain dorsal view of an *mpeg1*::*GAL4-UAS*::*Kaede*;*HB-NTR-mCherry* embryo, 24 hr after ventral photo-conversion and MTZ treatment. Invading cells deriving from the ventral region are in red/yellow.

(K) Number of hindbrain microglia in *mpeg1*::*GAL4-UAS*::*Kaede*;*HB-NTR-mCherry* embryos, 24 hr after ventral photo-conversion and drug treatment. Data are from three independent experiments.

HB, hindbrain; n, number of embryos; NS, non-significant; ***$p < 0.001$. NTR-mCherry^{+} neurons are in gray. Dotted line marks the hindbrain area or the embryo outline. Scale bar represents 30 μm.

indicated that, upon restoring nucleotide signaling, macrophages were able to migrate into the brain (Figures S4I–S4K).

Together these results provide compelling experimental support for a model where nucleotide signaling downstream of developmental neuronal apoptosis establishes the microglial population during embryonic brain formation by attracting committed precursors into the brain.

DISCUSSION

Many studies have focused on the origin of microglia and on their responses to pathological conditions (for a review see Prinz and Priller, 2014). However, little is known about the mechanisms responsible for establishing the microglial population in the embryo. Here we show that microglia exploit a physiological feature

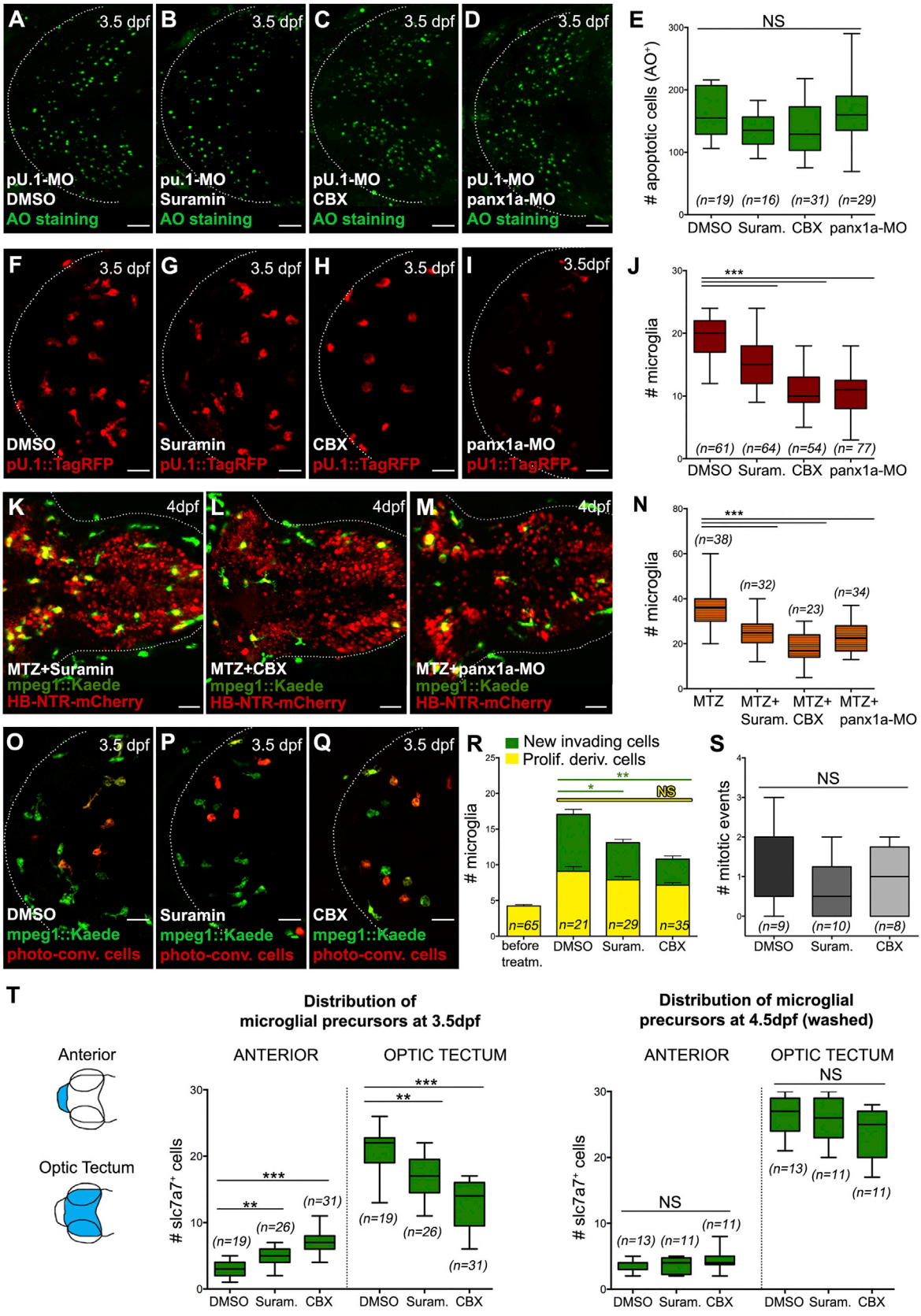

(legend on next page)

of normal brain development, namely, naturally occurring neuronal apoptosis. Accumulation of dying neurons in the developing brain contributes to the establishment of the microglial population by promoting both cell invasion and local proliferation. As microglia are the professional phagocytes of the brain and one of their main functions is the removal of apoptotic neurons, the existence of a link between the rate of neuronal cell death and the distribution of microglia provides a clear example of a function-based mechanism for microglial brain colonization. This is similar to other dynamic processes in which cells are organized in response to cues that depend on their function. Examples of this are vertebrate angiogenesis, where blood vessels are remodeled in response to blood flow (Yashiro et al., 2007), and terminal branching of the *Drosophila* trachea, where FGF expression is regulated by hypoxia to ensure that branches sprout toward oxygen-deprived areas (Ghabrial et al., 2003).

Importantly, our work provides experimental evidence of a role for developmental brain apoptosis in the long-term positioning of microglia. Obviously, this faction-based layer of control does not exclude the existence of other mechanisms that contribute to attracting and positioning microglia within the brain. For instance, in the mouse, the chemokines CXCL12 and CX3CL1 have been shown to be involved in the recruitment of microglia to specific brain areas, such as the sub-ventricular zone and the barrel centers, respectively (Arnò et al., 2014; Hoshiko et al., 2012).

The role of nucleotides in attracting microglial precursors into the brain identifies an interesting mechanistic link between development and pathology, as nucleotides also have been found to guide adult and embryonic microglia toward sites of damage (Davalos et al., 2005; Sieger et al., 2012; Haynes et al., 2006). Interestingly, it has been shown that nucleotides function as "find me" signals for the clearance of apoptotic cells (Elliott et al., 2009). In this regard, our work broadens this definition as we show that nucleotide-mediated chemotaxis is exploited to target tissue phagocytes to the developing brain. Not addressed here is the nature of the nucleotides that attract microglia and the underlying cellular mechanisms responsible for this attraction. Considering the presence of hydrolyzing ectonucleotidases in the extracellular space, formation of a stable long-range UTP/ATP gradient is unlikely. Instead, we favor a scenario where end products, such as adenosine, might work to recruit microglial precursors. Importantly, although we show that neuronal cell death promotes microglial proliferation, we did not observe a role for nucleotides in this context, as was suggested by in vitro experiments (Gebicke-Haerter et al., 1996; Bianco et al., 2006; Monif et al., 2009). This indicates that other signals might be involved in stimulating microglial cell division downstream of neuronal apoptosis.

Finally, this study identifies a new cell-non-autonomous role for developmental apoptosis. Traditionally known to control cell numbers, here programmed cell death regulates immune cell homing and the establishment of the immune-neuronal interface.

EXPERIMENTAL PROCEDURES

Fish Maintenance and Transgenic Lines

Zebrafish were kept at 26°C–27°C in a 14-hr light and 10-hr dark cycle. Embryos were collected by natural spawning and raised at 28.5°C in E3 buffer. To avoid pigmentation, 0.003% 1-phenyl-2-thiourea (PTU) was added at 1 dpf. Staging of embryos was done according to Kimmel et al. (1995). The transgenic lines *pU.1*::*Gal4-UAS*::*TagRFP*, *mpeg1*::*Gal4-UAS*::*Kaede*, *nbt*::*DlexPR*::*NTR-mCherry*, and *slc7a7*::*Kaede* were described previously (Sieger et al., 2012; Ellett et al., 2011; Mazaheri et al., 2014; Rossi et al., 2015). Animals were housed in the European Molecular Biology Laboratory (EMBL) animal facilities under veterinarian supervision and the guidelines of the European Commission, revised directive 2010/63/EU, and AVMA guidelines 2007.

Morpholino Knockdown

All morpholinos were obtained from Gene Tools and injected at the following concentrations: *pU.1*-MO, 0.5 mM (5′-GATATACTGATACTCCATTGGTG GT-3′; Rhodes et al., 2005); *caspase-3*-MO, 0.1 mM (5′-TTGCGTCCACACA GTCTCCGTTCAT-3′; Yamashita et al., 2008); *p53*-MO, 0.1 mM (5′-AGAATT GATTTTGCCGACCTCCTCT-3′; Rentzsch et al., 2003); and *panx1a*-MO, 1 mM (5′-CATATGTTGTATGCGCTTGCCTTAT-3′; Li et al., 2012).

Overexpression of *xiap* in Neurons

The coding sequence of zebrafish *xiap* was obtained from Source BioScience (LifeSciences) and amplified by PCR. This was cloned under the neuronal NBT promoter (Peri and Nüsslein-Volhard, 2008) and co-injected with or without the *pU.1*-MO (Rhodes et al., 2005).

Drug Treatments

All chemicals were purchased from Sigma-Aldrich and dissolved in E3 with DMSO at the following concentration: z-VAD-fmk, 300 μM; MTZ, 10 mM; CBX, 25 μM; and suramin, 5 mM.

Figure 4. Nucleotide Release Downstream of Neuronal Cell Death Recruits Microglial Precursors into the Brain

(A–E) AO staining (A–D) and quantification (E) of apoptotic nuclei in 4-dpf *pU.1*-morphant embryos, 24 hr after treatment with DMSO (A), suramin (B), CBX (C), and *pannexin1a*-MO (D), are shown.

(F–J) Microglial distribution (F–I) and quantification (J) in *pU.1*::*GAL4-UAS*::*TagRFP* embryos, 24 hr after treatment with DMSO (F), suramin (G), CBX (H), and *pannexin1a*-MO (I), are shown.

(K–N) Representative hindbrain (K–M) and quantification (N) of an *mpeg1*::*GAL4-UAS*::*Kaede*;*HB*::*NTR-mCherry* embryo at 4 dpf, 24 hr after treatment with MTZ + suramin (K), MTZ + CBX (L), and MTZ + *pannexin1a*-MO (M). Dotted lines mark the hindbrain.

(O–Q) Dorsal views of *mpeg1*::*GAL4-UAS*::*Kaede* embryos 24 hr after photo-conversion of microglia and treatment with DMSO (O), suramin (P), and CBX (Q). Newly entered microglia are in green. Microglia derived from converted cells are in red/yellow.

(R) Quantification of microglia deriving from cell invasion and in loco proliferation 24 hr after photo-conversion and drug treatment is shown.

(S) Quantification of mitotic events in the optic tectum of 2.5-dpf *mpeg1*::*GAL4-UAS*::*Kaede* embryos during ~15 hr of DMSO, suramin, or CBX treatment is shown.

(T) Number of *slc7a7*$^{+}$ microglial precursors accumulating in the anterior head region and in the optic tectum of *slc7a7*::*Kaede* embryos, 24 hr after drug treatment (graph on the left) and drug washout (graph on the right). Blue-colored areas in the schematic indicate the regions of interest.

For all quantifications, data are pooled from three independent experiments. Dotted line delimits the areas of interest. n, number of analyzed embryos; NS, non-significant; *p < 0.05, **p < 0.01, and ***p < 0.001. Scale bar represents 30 μm. See also Figures S3 and S4.

Induction of Brain Apoptosis

To induce apoptosis in the optic tectum, 3dpf *pU.1*::*Gal4-UAS*::*TagRFP* embryos were irradiated with a pulsed 355-nm laser coupled to the Andor Spinning Disk using a 20×/numerical aperture (NA) 0.7 objective. To ectopically induce neuronal cell death in the hindbrain, 3-day-old *nbt*::*DlexPR*::*NTR-mCherry* embryos were incubated with MTZ. After 24 hr embryos were rinsed extensively and kept in E3 buffer for further analysis.

Imaging and Kaede Photo-conversion

For live imaging, zebrafish embryos were anesthetized in 0.01% tricaine and embedded in 1.3% low-melting-point agarose. Imaging was performed using the Olympus FV1200 and Zeiss LSM780 with a 20×/NA 0.4 or a PlanApo 10×/0.25 objective. For full-brain and body imaging, we captured 30–40 z stacks, with a z step of 1.5–2 μm. Imaging of the *slc7a7*::*Kaede* line was performed with the Zeiss light sheet fluorescent microscope (Lightsheet Z.1) using a 20× water immersion objective. Images were analyzed in Imaris 7.6.4 (Bitplane). For photo-conversion of Kaede^{+} macrophages, *mpeg1*::*Gal4-UAS*::*Kaede* transgenic embryos were photo-converted using an Olympus FV1200 microscope equipped with a 405-nm laser. The following filter sets were used: unconverted Kaede (excitation at 488 nm and emission at 500–550 nm) and photo-converted Kaede (excitation at 559 nm and emission at 570–600 nm).

For serial photo-conversion of microglia, Kaede^{+} cells found in the optic tectum were photo-converted at 2.5, 3.5, 4.5, or 5.5 dpf, and the numbers of green and red/yellow cells were quantified 24 hr after each round of photo-conversion.

Photo-converted *mpeg1*::*Gal4-UAS*::*Kaede*;*nbt*::*DlexPR*::*NTR-mCherry* embryos were imaged with Olympus FV1200 using the virtual channel tool with the following filter sets: unconverted Kaede (excitation at 488 nm and emission at 500–550 nm), photo-converted Kaede (excitation at 559 nm and emission at 570–600 nm), and mCherry (excitation at 559 nm and emission at 630–730 nm).

SUPPLEMENTAL INFORMATION

Supplemental Information includes Supplemental Experimental Procedures, four figures, and one movie and can be found with this article online at http://dx.doi.org/10.1016/j.celrep.2016.06.033.

AUTHOR CONTRIBUTIONS

A.M.C. designed the study, conducted the experiments, and analyzed the data. M.A. carried out microglial segmentation and density analysis in juvenile brains. F.P. designed the study and wrote the manuscript with A.M.C.

ACKNOWLEDGMENTS

We are grateful to the EMBL Advanced Light Microscopy Facility for assistance with microscope imaging. We would like to thank Olympus Europe for continuous support of the Advanced Light Microscopy Facility. We are grateful to A. Martin-Villalba, A. Aulehla, and P. Lénárt for critical discussion and D. Gilmour, S. Komoto, J. Benjaminsen, N. Norlin, O. Breus, K. Richter, and A. Villani for critical discussion and reading of the manuscript. This work was supported by funds from EMBL to A.M.C., M.A., and F.P.

Received: November 30, 2015
Revised: April 11, 2016
Accepted: June 3, 2016
Published: July 14, 2016

REFERENCES

Arnò, B., Grassivaro, F., Rossi, C., Bergamaschi, A., Castiglioni, V., Furlan, R., Greter, M., Favaro, R., Comi, G., Becher, B., et al. (2014). Neural progenitor cells orchestrate microglia migration and positioning into the developing cortex. Nat. Commun. *5*, 5611.

Bianco, F., Ceruti, S., Colombo, A., Fumagalli, M., Ferrari, D., Pizzirani, C., Matteoli, M., Di Virgilio, F., Abbracchio, M.P., and Verderio, C. (2006). A role for P2X7 in microglial proliferation. J. Neurochem. *99*, 745–758.

Casano, A.M., and Peri, F. (2015). Microglia: multitasking specialists of the brain. Dev. Cell *32*, 469–477.

Chekeni, F.B., Elliott, M.R., Sandilos, J.K., Walk, S.F., Kinchen, J.M., Lazarowski, E.R., Armstrong, A.J., Penuela, S., Laird, D.W., Salvesen, G.S., et al. (2010). Pannexin 1 channels mediate 'find-me' signal release and membrane permeability during apoptosis. Nature *467*, 863–867.

Chen, S.K., Tvrdik, P., Peden, E., Cho, S., Wu, S., Spangrude, G., and Capecchi, M.R. (2010). Hematopoietic origin of pathological grooming in Hoxb8 mutant mice. Cell *141*, 775–785.

Curado, S., Anderson, R.M., Jungblut, B., Mumm, J., Schroeter, E., and Stainier, D.Y.R. (2007). Conditional targeted cell ablation in zebrafish: a new tool for regeneration studies. Dev. Dyn. *236*, 1025–1035.

Davalos, D., Grutzendler, J., Yang, G., Kim, J.V., Zuo, Y., Jung, S., Littman, D.R., Dustin, M.L., and Gan, W.-B. (2005). ATP mediates rapid microglial response to local brain injury in vivo. Nat. Neurosci. *8*, 752–758.

Dekkers, M.P.J., Nikoletopoulou, V., and Barde, Y.-A. (2013). Cell biology in neuroscience: Death of developing neurons: new insights and implications for connectivity. J. Cell Biol. *203*, 385–393.

Deveraux, Q.L., Takahashi, R., Salvesen, G.S., and Reed, J.C. (1997). X-linked IAP is a direct inhibitor of cell-death proteases. Nature *388*, 300–304.

Ellett, F., Pase, L., Hayman, J.W., Andrianopoulos, A., and Lieschke, G.J. (2011). mpeg1 promoter transgenes direct macrophage-lineage expression in zebrafish. Blood *117*, e49–e56.

Elliott, M.R., Chekeni, F.B., Trampont, P.C., Lazarowski, E.R., Kadl, A., Walk, S.F., Park, D., Woodson, R.I., Ostankovich, M., Sharma, P., et al. (2009). Nucleotides released by apoptotic cells act as a find-me signal to promote phagocytic clearance. Nature *461*, 282–286.

Gebicke-Haerter, P.J., Christoffel, F., Timmer, J., Northoff, H., Berger, M., and Van Calker, D. (1996). Both adenosine A1- and A2-receptors are required to stimulate microglial proliferation. Neurochem. Int. *29*, 37–42.

Ghabrial, A., Luschnig, S., Metzstein, M.M., and Krasnow, M.A. (2003). Branching morphogenesis of the Drosophila tracheal system. Annu. Rev. Cell Dev. Biol. *19*, 623–647.

Ginhoux, F., Greter, M., Leboeuf, M., Nandi, S., See, P., Gokhan, S., Mehler, M.F., Conway, S.J., Ng, L.G., Stanley, E.R., et al. (2010). Fate mapping analysis reveals that adult microglia derive from primitive macrophages. Science *330*, 841–845.

Ginhoux, F., Lim, S., Hoeffel, G., Low, D., and Huber, T. (2013). Origin and differentiation of microglia. Front. Cell. Neurosci. *7*, 45.

Gomez Perdiguero, E., Klapproth, K., Schulz, C., Busch, K., Azzoni, E., Crozet, L., Garner, H., Trouillet, C., de Bruijn, M.F., Geissmann, F., and Rodewald, H.R. (2015). Tissue-resident macrophages originate from yolk-sac-derived erythro-myeloid progenitors. Nature *518*, 547–551.

Haynes, S.E., Hollopeter, G., Yang, G., Kurpius, D., Dailey, M.E., Gan, W.B., and Julius, D. (2006). The P2Y12 receptor regulates microglial activation by extracellular nucleotides. Nat. Neurosci. *9*, 1512–1519.

Herbomel, P., Thisse, B., and Thisse, C. (2001). Zebrafish early macrophages colonize cephalic mesenchyme and developing brain, retina, and epidermis through a M-CSF receptor-dependent invasive process. Dev. Biol. *238*, 274–288.

Hoshiko, M., Arnoux, I., Avignone, E., Yamamoto, N., and Audinat, E. (2012). Deficiency of the microglial receptor CX3CR1 impairs postnatal functional development of thalamocortical synapses in the barrel cortex. J. Neurosci. *32*, 15106–15111.

Kierdorf, K., Erny, D., Goldmann, T., Sander, V., Schulz, C., Perdiguero, E.G., Wieghofer, P., Heinrich, A., Riemke, P., Hölscher, C., et al. (2013). Microglia emerge from erythromyeloid precursors via Pu.1- and Irf8-dependent pathways. Nat. Neurosci. *16*, 273–280.

Kimmel, C.B., Ballard, W.W., Kimmel, S.R., Ullmann, B., and Schilling, T.F. (1995). Stages of embryonic development of the zebrafish. Dev. Dyn. *203*, 253–310.

Kizil, C., Dudczig, S., Kyritsis, N., Machate, A., Blaesche, J., Kroehne, V., and Brand, M. (2012). The chemokine receptor cxcr5 regulates the regenerative neurogenesis response in the adult zebrafish brain. Neural Dev. *7*, 27.

Kroehne, V., Freudenreich, D., Hans, S., Kaslin, J., and Brand, M. (2011). Regeneration of the adult zebrafish brain from neurogenic radial glia-type progenitors. Development *138*, 4831–4841.

Li, Y., Du, X.F., Liu, C.S., Wen, Z.L., and Du, J.L. (2012). Reciprocal regulation between resting microglial dynamics and neuronal activity in vivo. Dev. Cell *23*, 1189–1202.

Mazaheri, F., Breus, O., Durdu, S., Haas, P., Wittbrodt, J., Gilmour, D., and Peri, F. (2014). Distinct roles for BAI1 and TIM-4 in the engulfment of dying neurons by microglia. Nat. Commun. *5*, 4046.

Monif, M., Reid, C.A., Powell, K.L., Smart, M.L., and Williams, D.A. (2009). The P2X7 receptor drives microglial activation and proliferation: a trophic role for P2X7R pore. J. Neurosci. *29*, 3781–3791.

Nijhawan, D., Honarpour, N., and Wang, X. (2000). Apoptosis in neural development and disease. Annu. Rev. Neurosci. *23*, 73–87.

Parkhurst, C.N., Yang, G., Ninan, I., Savas, J.N., Yates, J.R., 3rd, Lafaille, J.J., Hempstead, B.L., Littman, D.R., and Gan, W.B. (2013). Microglia promote learning-dependent synapse formation through brain-derived neurotrophic factor. Cell *155*, 1596–1609.

Peri, F., and Nüsslein-Volhard, C. (2008). Live imaging of neuronal degradation by microglia reveals a role for v0-ATPase a1 in phagosomal fusion in vivo. Cell *133*, 916–927.

Pisharath, H., Rhee, J.M., Swanson, M.A., Leach, S.D., and Parsons, M.J. (2007). Targeted ablation of beta cells in the embryonic zebrafish pancreas using E. coli nitroreductase. Mech. Dev. *124*, 218–229.

Prinz, M., and Priller, J. (2014). Microglia and brain macrophages in the molecular age: from origin to neuropsychiatric disease. Nat. Rev. Neurosci. *15*, 300–312.

Rentzsch, F., Kramer, C., and Hammerschmidt, M. (2003). Specific and conserved roles of TAp73 during zebrafish development. Gene *323*, 19–30.

Rhodes, J., Hagen, A., Hsu, K., Deng, M., Liu, T.-X., Look, A.T., and Kanki, J.P. (2005). Interplay of pu.1 and gata1 determines myelo-erythroid progenitor cell fate in zebrafish. Dev. Cell *8*, 97–108.

Rossi, F., Casano, A.M., Henke, K., Richter, K., and Peri, F. (2015). The SLC7A7 transporter identifies microglial precursors prior to entry into the brain. Cell Rep. *11*, 1008–1017.

Sandilos, J.K., Chiu, Y.H., Chekeni, F.B., Armstrong, A.J., Walk, S.F., Ravichandran, K.S., and Bayliss, D.A. (2012). Pannexin 1, an ATP release channel, is activated by caspase cleavage of its pore-associated C-terminal autoinhibitory region. J. Biol. Chem. *287*, 11303–11311.

Sieger, D., Moritz, C., Ziegenhals, T., Prykhozhij, S., and Peri, F. (2012). Long-range Ca^{2+} waves transmit brain-damage signals to microglia. Dev. Cell *22*, 1138–1148.

Sierra, A., Abiega, O., Shahraz, A., and Neumann, H. (2013). Janus-faced microglia: beneficial and detrimental consequences of microglial phagocytosis. Front. Cell. Neurosci. *7*, 6.

Stachura, D.L., and Traver, D. (2011). Cellular dissection of zebrafish hematopoiesis. Methods Cell Biol. *101*, 75–110.

Svahn, A.J., Graeber, M.B., Ellett, F., Lieschke, G.J., Rinkwitz, S., Bennett, M.R., and Becker, T.S. (2013). Development of ramified microglia from early macrophages in the zebrafish optic tectum. Dev. Neurobiol. *73*, 60–71.

van Ham, T.J., Brady, C.A., Kalicharan, R.D., Oosterhof, N., Kuipers, J., Veenstra-Algra, A., Sjollema, K.A., Peterson, R.T., Kampinga, H.H., and Giepmans, B.N. (2014). Intravital correlated microscopy reveals differential macrophage and microglial dynamics during resolution of neuroinflammation. Dis. Model. Mech. *7*, 857–869.

von Kügelgen, I. (2008). Pharmacology of mammalian P2X- and P2Y-receptors. Biotrend Rev. *3*, 1–12.

Williams, J.A., and Holder, N. (2000). Cell turnover in neuromasts of zebrafish larvae. Hear. Res. *143*, 171–181.

Xu, J., Du, L., and Wen, Z. (2012). Myelopoiesis during zebrafish early development. J. Genet. Genomics *39*, 435–442.

Xu, J., Zhu, L., He, S., Wu, Y., Jin, W., Yu, T., Qu, J.Y., and Wen, Z. (2015). Temporal-spatial resolution fate mapping reveals distinct origins for embryonic and adult microglia in zebrafish. Dev. Cell *34*, 632–641.

Yamashita, M., Mizusawa, N., Hojo, M., and Yabu, T. (2008). Extensive apoptosis and abnormal morphogenesis in pro-caspase-3 transgenic zebrafish during development. J. Exp. Biol. *211*, 1874–1881.

Yashiro, K., Shiratori, H., and Hamada, H. (2007). Haemodynamics determined by a genetic programme govern asymmetric development of the aortic arch. Nature *450*, 285–288.